CHARACTERIZATION OF SMALL MOLECULE INHIBITORS OF CLKS AND DYRKS

by

Lucia Gonzalez

A Thesis Submitted to the Faculty of the

DEPARTMENT OF CELLULAR AND MOLECULAR MEDICINE PROGRAM

In Partial Fulfillment of the Requirements

For the Degree of

Master of Science

In the Graduate College

THE UNIVERSITY OF ARIZONA

2023

THE UNIVERSITY OF ARIZONA
GRADUATE COLLEGE

As members of the Master's Committee, we certify that we have read the thesis prepared by Lucia Gonzalez, titled *Characterization of Small Molecule Inhibitors of CLKs and DYRKs* and recommend that it be accepted as fulfilling the dissertation requirement for the Master's Degree.

Dr. Curtis Thorne — Date: 10/27/23

Dr. Andrew Paek — Date: 10/27/23

Dr. Justin E. Wilson — Date: 10/27/23

Final approval and acceptance of this thesis is contingent upon the candidate's submission of the final copies of the thesis to the Graduate College.

I hereby certify that I have read this thesis prepared under my direction and recommend that it be accepted as fulfilling the Master's requirement.

Dr. Curtis Thorne — Date: 10/27/23
Master's Thesis Committee Chair
Department of Cellular and Molecular Medicine

Table of Contents

List of Figures

List of Tables

Abstract

Colorectal cancer (CRC) used to be known as a disease of old age, but now it is becoming a concern for younger adults. Researchers are unsure why, but they believe it may be due to environmental factors that lead to genetic changes in the colonic epithelium. These genetic changes affect essential signaling pathways, making them a crucial research focus. The Wnt signaling pathway is significant in maintaining digestive tract homeostasis but is often dysregulated in cancer. For this reason, researchers are working to identify proteins that affect Wnt signaling and target them with inhibitors. The CLK and DYRK kinase families are a group of proteins closely linked to the Wnt signaling pathway and implicated in disease. In this study, I tested 107 novel small molecules that are CLK/DYRK inhibitors in a dose-response curve with human colonic epithelial cells (HCECs). From this data, we identified six top compounds that were tested further in a cell viability assay to determine their efficacy against cancer cells. We also immunoblotted for CLKs' substrate to understand how the compounds work and obtained pharmacokinetic data to understand their biomechanics. Ultimately, two promising compounds emerged as potential candidates for further organoid profiling – DYR726 and DYR895. We are especially excited for DYR895 to be FDA-approved soon, but we will also further assess DYR726.

Introduction

In 2020, there were over 2 million colorectal cancer (CRC) cases worldwide. CRC was declared the second leading cause of cancer-related deaths in the same year (WHO, 2023). In the United States, CRC is expected to claim approximately 53,000 lives by the end of 2023, primarily affecting American Indians, Alaskan Natives, and African Americans (ACS, 2023). Genetics and behavioral factors play a significant role in the development of CRC. Risk factors for CRC include obesity, adopting a sedentary lifestyle, high consumption of red meat and processed food, and finally, alcohol abuse and smoking. The development of cancer involves the acquisition of a hallmark of cellular behaviors. One of the ways the disease obtains these hallmarks is through the progressive accumulation of genetic mutations that cause the loss of genetic stability by inactivating DNA repair mechanisms (Kuipers et al., 2015). Although CRC cases caused by inherited germline mutations have decreased due to preventative screening geared toward older adults, somatic mutations are rising in young adults. Sporadic CRC cases pertain to nearly three-quarters of patients without family history (Kuipers et al., 2015). Mortality rates are alarming, yet prevalence rates are declining due to routine screening. Still, there is more to uncover to understand the progression of CRC. Signal pathway research has become very relevant to further expose target therapies for CRC. The Wnt signaling pathway is a significant conductor concerning the epithelia in the digestive tract and CRC.

The colon is the final division of the digestive tract, in which mostly water absorption and waste management and elimination take place. The lining of the colon –and most of the digestive tract– comprises columnar epithelia, which forms a barrier between the

colon's lumen and the inside of the body. The colon has evolved into measuring up to 4.9 feet and organizes itself into invaginations called crypts to maximize absorption. At the base of the crypts exists a group of stem cells that maintain the organization of the colon epithelia and are the driving force of cell renewal and differentiation. Stem cells may differentiate into absorptive, goblet, enteroendocrine, transit-amplifying, and Paneth cells (Figure 1). They renew meticulously and are directed by molecular and cellular communication via the Wnt signaling pathway. Diseases like cancer may arise when mutations occur, directly and indirectly affecting the Wnt pathway.

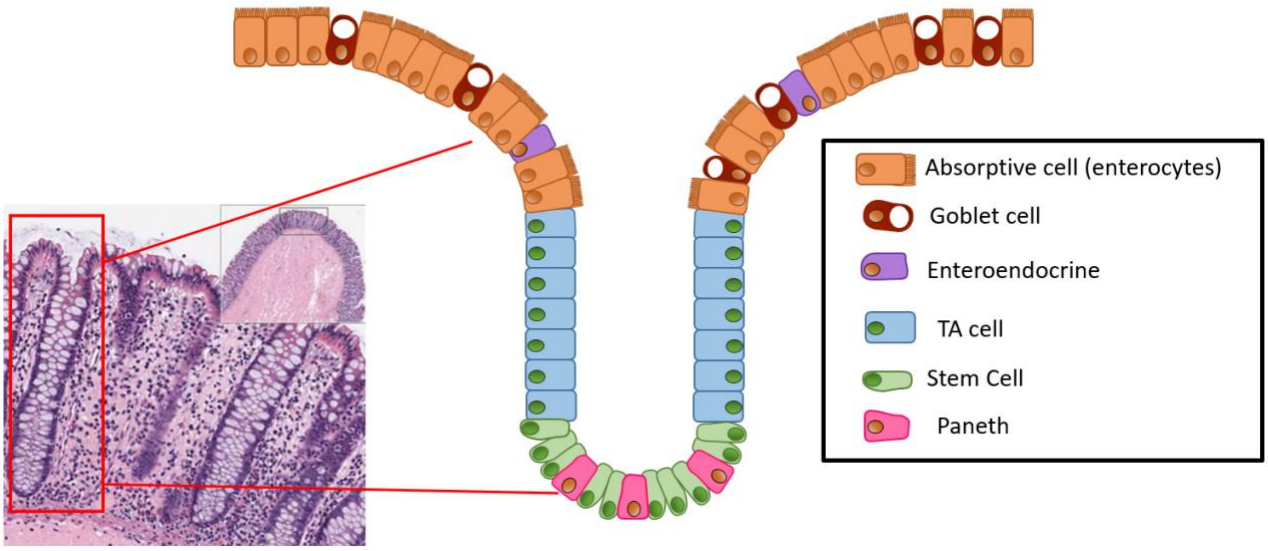

Figure 1. The Digestive Tract Epithelium

Crypts in the colon comprise a stem cell niche in which cells can replicate into other stem cells or differentiate into other types of cells. Transit-amplifying cells are stem cells in transition to become enterocytes, goblet, or enteroendocrine cells, which form the barrier of the lumen of the digestive tract and inside of the body.

The Wnt signaling pathway is an evolutionarily conserved cellular mechanism crucial in developmental gene expression programs involved in stem cell proliferation and self-

renewal. The term ‘Wnt’ was coined to refer to homologous proteins in *Drosophila* (Wg) and mice (Int-1) by Nusse et al. in 1991. Two major pathways involve Wnt signaling: canonical (β-catenin protein-dependent) and non-canonical (β-catenin protein-independent). This thesis will focus on the canonical Wnt pathway, defined by the cytosolic accumulation of β-catenin, resulting in its migration to the nucleus to regulate target gene expression. Without a Wnt ligand, β-catenin is degraded in the proteasome after phosphorylation by the β-catenin destruction complex –hence its name. The β-catenin destruction complex is composed of axin (a scaffolding protein), APC (Adenomatous polyposis coli), CK1 (Casein kinase 1), and GSK3 (Glycogen synthase kinase 3). When a Wnt ligand is present, it binds to Frizzled (Fz), a seven-pass transmembrane receptor, and its co-receptor LRP5/6 (low-density lipoprotein receptor-related) (Nusse, 2023). This Wnt-Fz-LRP5/6 complex recruits the protein, Dishevelled (Dsh), to phosphorylate LRP5/6 to recruit the destruction complex and disable it. Without the active destruction complex, β-catenin accumulates and reaches the nucleus. In the nucleus β-catenin displaces Groucho, a corepressor nuclear factor, and binds to the transcription factor, TCF (T-cell factor), to act as a co-inducer to stimulate Wnt target genes (MacDonald et al., 2009) (Figure 2). This simple explanation of the Wnt signaling pathway should not minimize its complexity. Researchers, us, have yet to study more of its complex molecular interrelations, including that in which its hyperactivation is believed to be CRC's initiating and driving event (Schatoff et al., 2017).

Along with the Wnt signaling pathway, we are highly interested in protein kinases. A kinase is a key signaling enzyme that phosphorylates protein targets. In detail, kinases catalyze the transfer of phosphate from ATP (or GTP) to its protein substrate. Along with

phosphatases, kinases are responsible for phosphorylating 30% of cellular proteins (Cheng et al., 2011). Through phosphorylation, kinases regulate protein functions by inducing conformational changes or disrupting and creating protein-protein interaction motifs. There are over 500 kinases in the human kinome. The family of CDC-like kinases (CLKs) and the Dual-specificity tyrosine phosphorylation-regulated kinases (DYRKs) are two groups of many that are highly involved with the Wnt signaling pathway, specifically in the context of the colon and CRC.

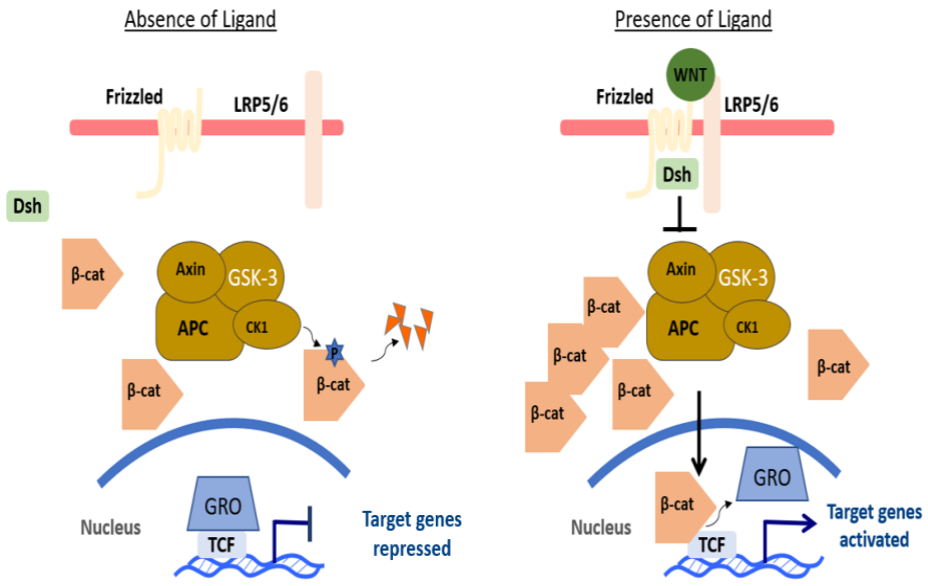

Figure 2. Wnt Signaling Pathway

In the absence of a Wnt ligand, B-catenin is phosphorylated by GSK3 and CK1 in the β-catenin destruction complex to be sent for degradation by the proteasome. This prevents the expression of target genes necessary for proliferation and differentiation. The presence of a Wnt ligand allows the binding of the Wnt-Frizzled-LRP5/6 complex to recruit Dischevelled (Dsh) to act on the destruction complex and disable it. Disabling the destruction complex allows β-catenin to accumulate and translocate into the nucleus to displace Groucho (GRO), bind to TCF, and allow target gene transcription.

The CLKs and DYRKS are highly conserved kinases and highly similar in structure. Both families are usually sensitive to the same pharmacological inhibitors and, therefore usually jointly researched (Linberg et al., 2021). Both families of kinases are involved in many cellular functions, such as intracellular signaling, mRNA splicing, chromatin transcription, DNA damage repair, cell survival, and cell cycle control (Linberg et al., 2021). The CLK family can phosphorylate serine/threonine residues in other proteins and tyrosine residues on each other. It is suggested that CLKs' essential role involves the phosphorylation of serine and arginine-rich proteins (SR proteins), which are essential in regulating alternative splicing, which is pivotal for gene expression (Aubol et al., 2013). An increased diversity of the full range of mRNA expressed by an organism can be achieved by alternative splicing, leading to an increased diversity of proteins. Since regular phosphorylation of the CLK and DYRK families suggests normal cell processes, it would make sense that abnormal activities of the two families would lead to disease. It has been suggested that abnormal function of the CLK family is linked to glioblastomas and lung cancer (CLK1), autism and breast cancer (CLK2), prostate cancer and cholangiocarcinoma (CLK3), and more (Linberg et al., 2021). The CLKs specifically play a crucial role in regulating transcript splicing via the phosphorylation of SR proteins (SRSF1–12) (Song et al., 2023). Overall, CLK3 is relatively understudied compared to other members of the CLK family.

Our interest in CLK3 is based on a previous kinome-wide RNAi screen in 2015 to identify kinases highly involved with the Wnt signaling pathway. In that screen, our team knocked down each kinase individually from human colonic epithelial cells (HCECs) and followed with Wnt signaling stimulation. The kinase knockdown that led to the most

significant suppression of cell viability was caused by CLK3 when Wnt signaling was added. The CLK3 phenotype showed increased cell toxicity when Wnt signaling was activated compared to cells without Wnt signaling activation (Thorne et al., 2015; Cabel, 2023). Also, through literature research, we found that CLK3 has been declared an unfavorable marker when highly expressed in all stages of CRC. The higher CLK3 is expressed in CRC tumors, the lower the probability of survival of patients (Human Protein Atlas). With this information in hand, we set out to examine CLK3, which is widely recognized as understudied, and it is even on the NIH's official list of "dark kinases" (Berginski et al., 2021). Many questions arose, like: Could CLK3 be a proto-oncogenic? Could CLK3 be the cause of the observed poor prognosis of CRC patients?

Through years of research, we have discovered that CLK3 regulates the Wnt signaling pathways at the levels of signaling, transcription, mRNA splicing, and cell-cell adhesions (Cable, 2023). Because dysregulation of the Wnt signaling pathway in CRC is the root cause of cancer cell survival and proliferation and the fact that this dysregulation may be mediated by increased CLK3, targeting the Wnt signaling pathway via the CLK family could be a promising therapeutic target. In collaboration with the Hulme lab, a medicinal chemistry group from the College of Pharmacy at the University of Arizona, we have taken on the task of testing their novel small molecules that inhibit CLKs and DYRKs. In this thesis, I will test over a hundred novel small molecules to characterize them as pan-CLK/DYRK inhibitors based on their ability to inhibit Wnt target genes. The goal is to find the most potent small molecules that suppress Wnt target genes via inhibition of the CLK family by utilizing them in a cell-base assay designed to measure Wnt-mediated transcription, a cell viability assay, and immunoblotting. This report displays a set of small

molecules that will establish a baseline for compounds that can be pushed over to IND-enabling studies that include further *in vitro* and *in vivo* tests to help define the pharmacological and toxicological properties of the best-performing small molecules to inhibit Wnt target genes and treat CRC.

Results

Inhibition of Wnt Target Genes by Pan CLK/DYRK Inhibitors.

To determine if the molecules provided by the Hulme lab inhibit Wnt target genes, we used the Wnt reporter assay on HCECs with TopGFP reporter. HCECs were treated with an 11-dose response curve of the pan-CLK/DYR inhibitors in the presence and absence of CHIR99021, a GSK3 inhibitor, and thus a Wnt gene activator. Cells were stained for DAPI and imaged on a Nikon Ti2 Eclipse fluorescent microscope using wavelengths of 395 for DAPI, 488 for GFP, and 561 for mCherry. Single-cell analysis was performed using Nikon Elements software. Nuclei were segmented based on DAPI images. Also, single-cell object intensities were obtained for TopGFP and mCherry (HCECs internal control). Wnt activation was calculated by dividing the mean intensity of TopGFP by the mean intensity of mCherry. The data obtained was graphed using Jupyter and GraphPad Prism 10. TopGFP curves were plotted as arbitrary unit percentages in which 100% represents the average of TopGFP in the positive control (CHIR stimulation, no compound) and 0% represents the average of TopGFP in the negative control (DMSO, no CHIR). Nonlinear regressions for every compound were calculated, and EC50 curves were plotted. A few compounds reduced TopGFP expression significantly at low concentrations compared to others. Compounds DYR810, DYR825, DYR895, and DYR899 reduced half of TopGFP at the lowest concentrations, while other compounds

did not reduce TopGFP down to basal DMSO control conditions, such as DYR815, DYR827, and DYR861 (Figure 3).

Cell count analyses at every concentration were performed by segmenting the nuclei using DAPI. Cell count analysis determines the EC50, which measures the concentration of a compound inducing cell death halfway between the baseline and maximum. By evaluating the EC50s of cell count, we could determine if the inhibition of the Wnt pathway caused the decrease of TopGFP or if it was from cell toxicity caused by higher concentrations of the compounds. We disregarded compounds like DYR867, which had an excellent TopGFP EC50 but a high cell count EC50. Based on the cell count analysis on compound DYR867, we deduced that most of the inhibition of TopGFP was due to cell death caused by compound toxicity (Figure 4). Ultimately, the top compounds found to inhibit Wnt signaling without the influence of cell death potently were DYR810, DYR825, DYR860, DYR895, and DYR899 with TopGFP EC50s of 0.0036 μM, 0.0145 μM, 0.0051 μM and 0.0090 μM, respectively. These five compounds were added to a list of other potent small molecules previously tested by a predecessor and other researchers (DYR682 (Cirtuvivint), DYR726, and DYR747 with TopGFP EC50s of 0.0204 μM, 0.0407 μM and 0.0060 μM respectively) (Table 1).

TopGFP Analysis (DYR800-DYR841)

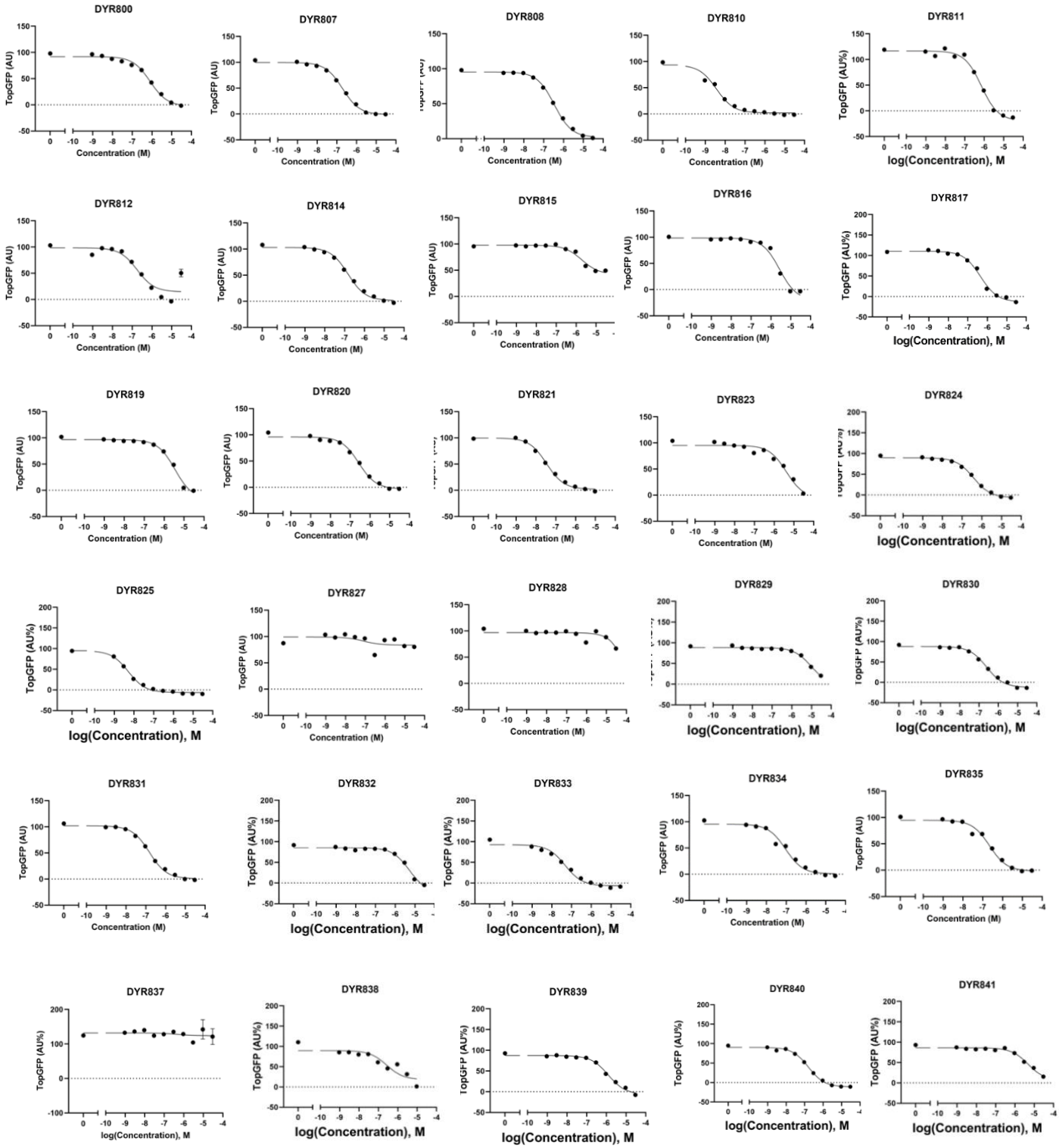

TopGFP Analysis (DYR842-DYR877)

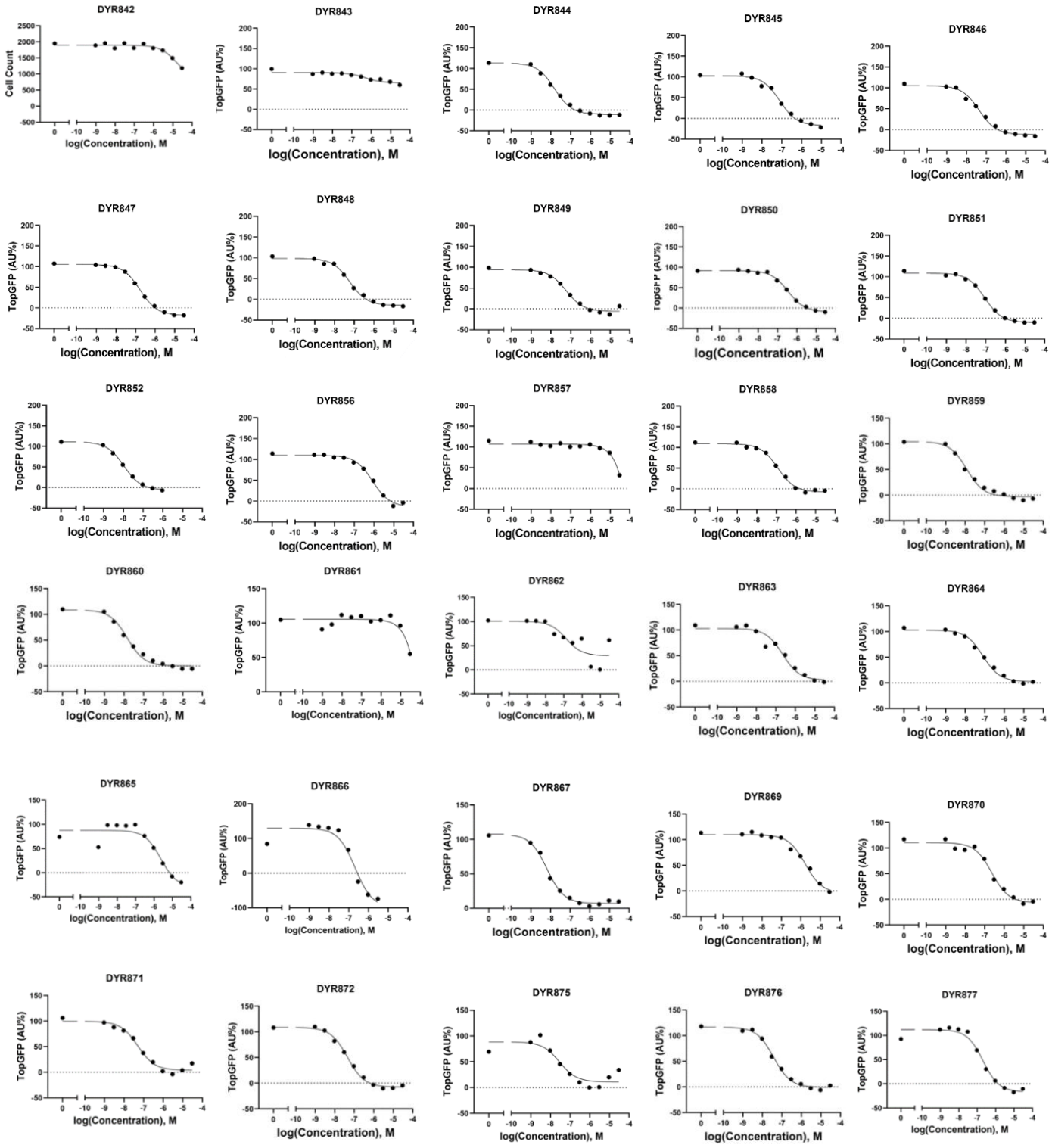

TopGFP Analysis (DYR878-DYR911)

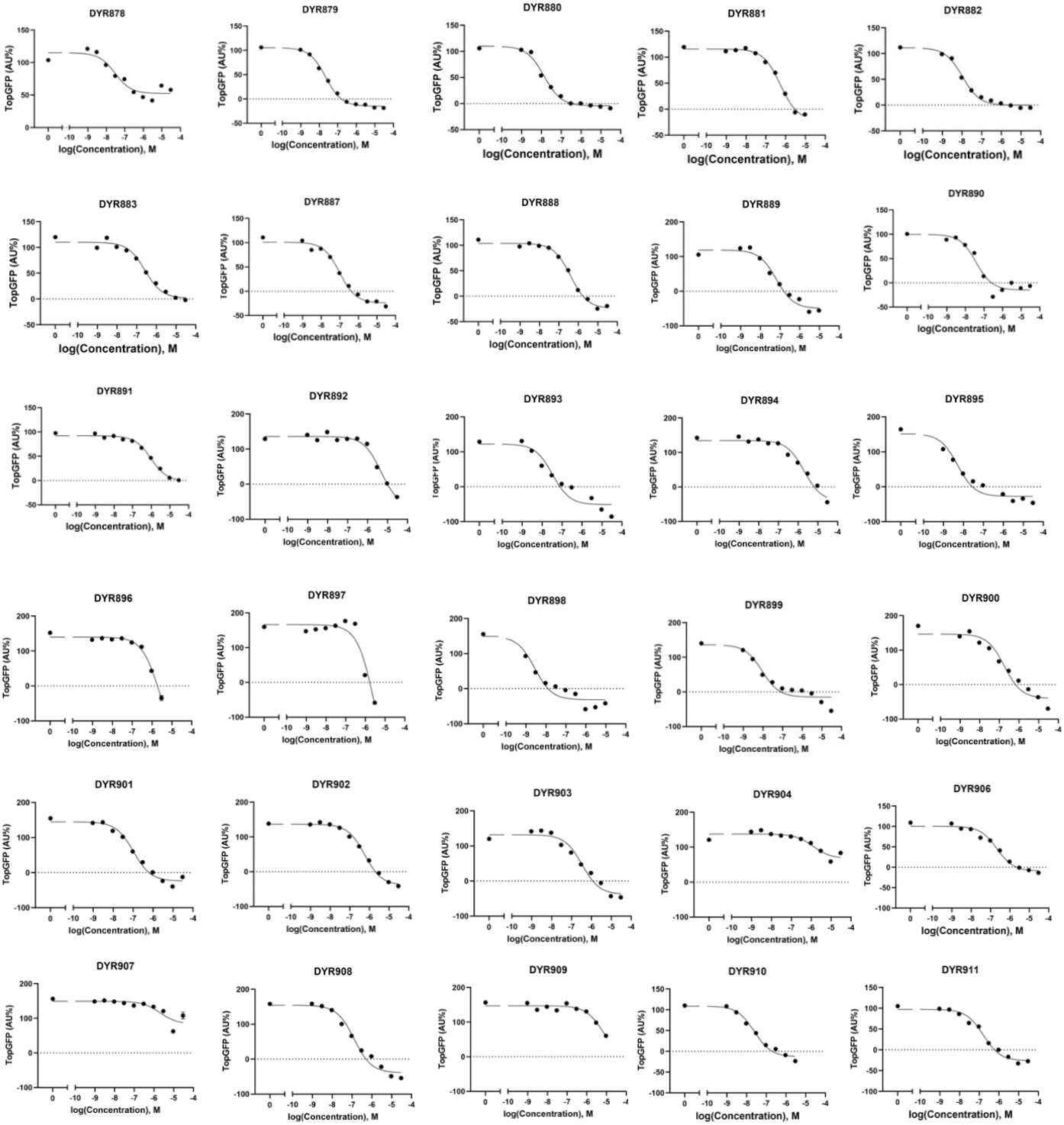

TopGFP Analysis (DYR912-CPD-A)

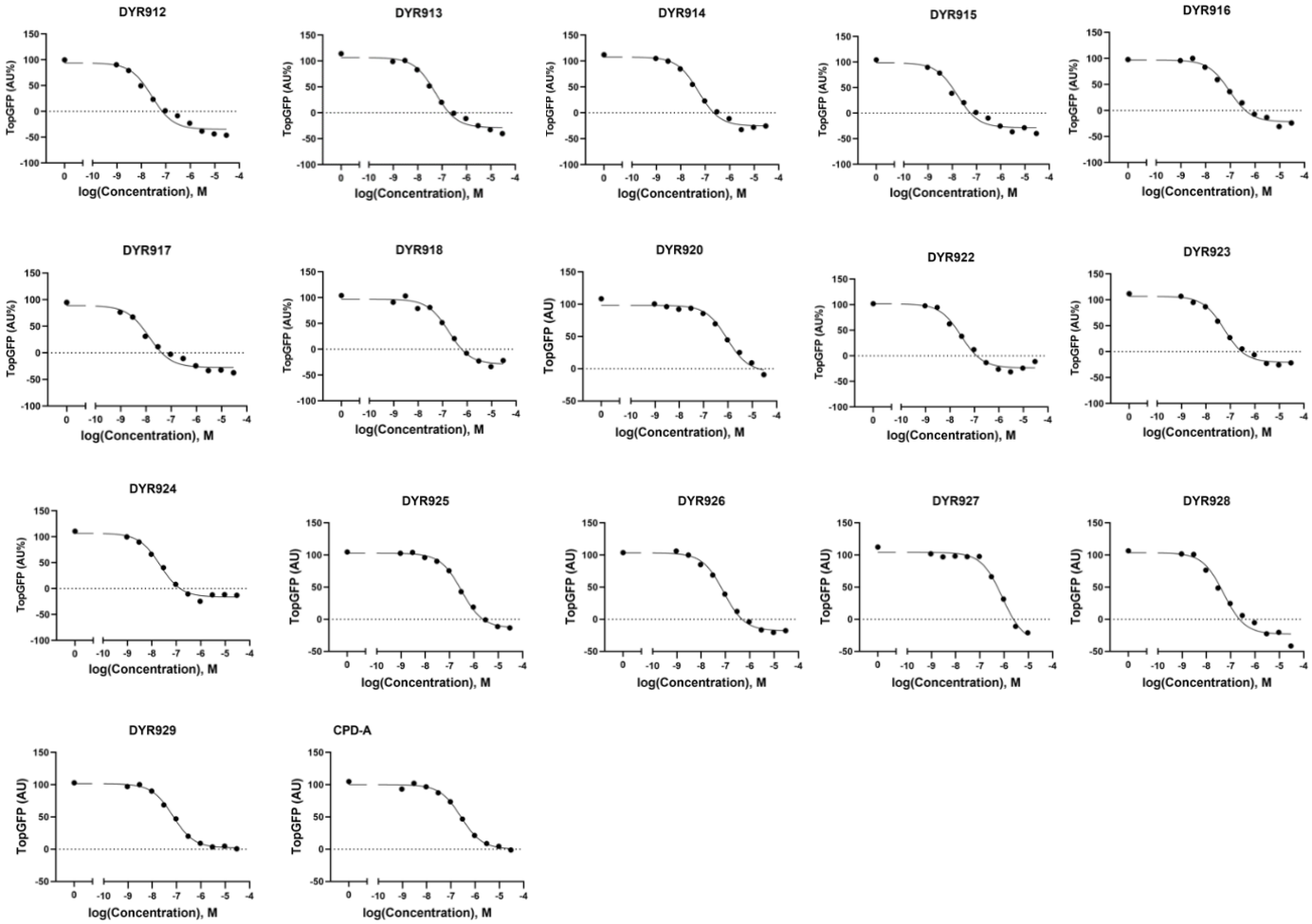

Figure 3. Pan-CLK/DYRK Inhibitors Downregulate Wnt Target Genes

HCECs with TopGFP reporter were treated with 11-dose-response curves of a library of 107 molecules synthesized by the Hulme lab at the University of Arizona. The dosages ranged from 30μM to 0μM, and half of the cells were stimulated with 10μM CHIR99021. Cells were fixed and stained to visualize the nuclei on a Nikon Ti2 Eclipse microscope. Nuclear GFP and mCherry were measured on the single-cell level using Nikon Elements, and such data was plotted using Jupyter and GraphPad Prism 10. Graphs above are plots of TopGFP as a percent response where 100 represents CHIR stimulation without a compound (positive control group), and 0 represents DMSO stimulation without the presence of a compound (negative control group).

Cell Count Analysis (DYR800-DYR841)

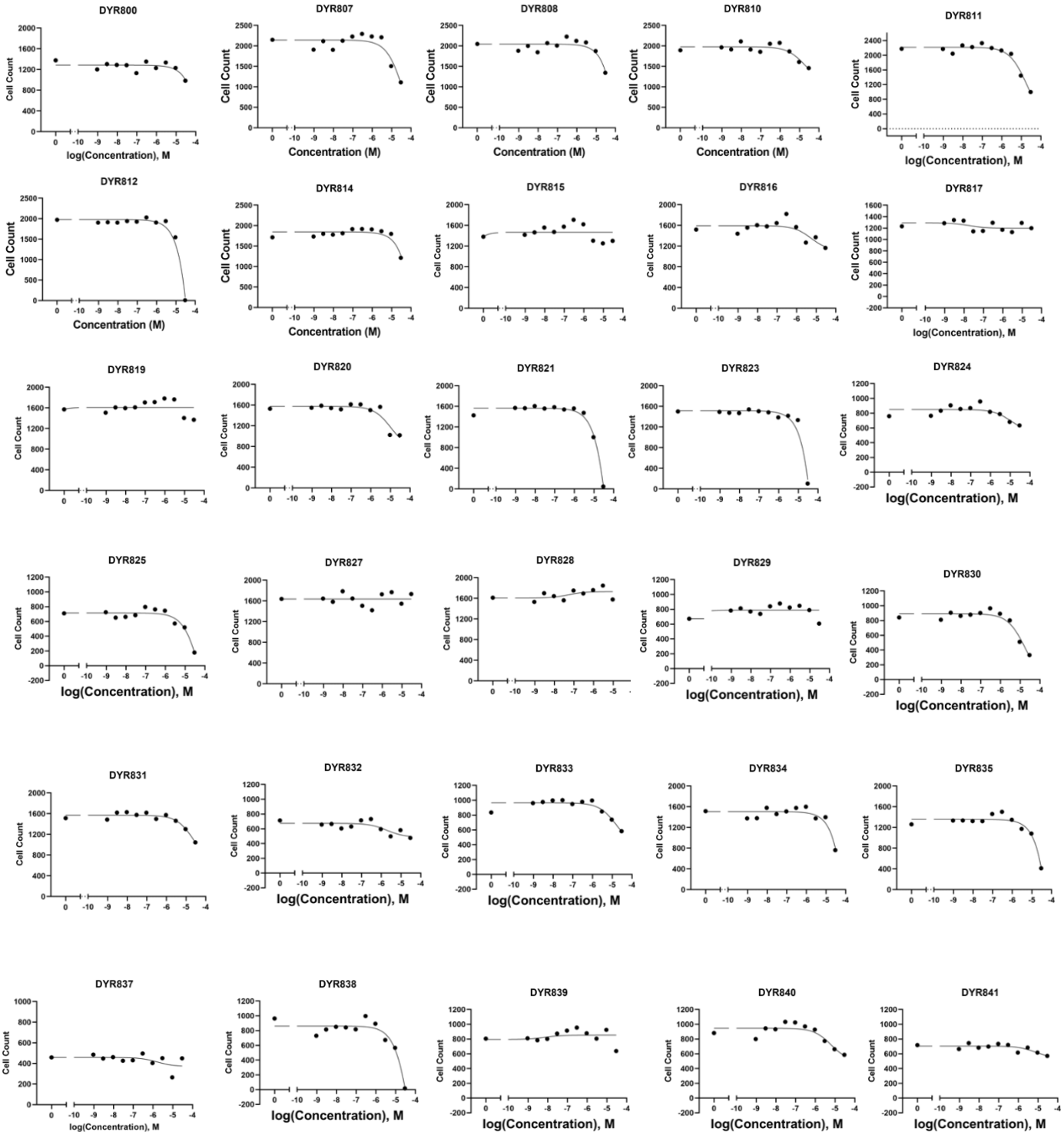

Cell Count Analysis (DYR842-DYR877)

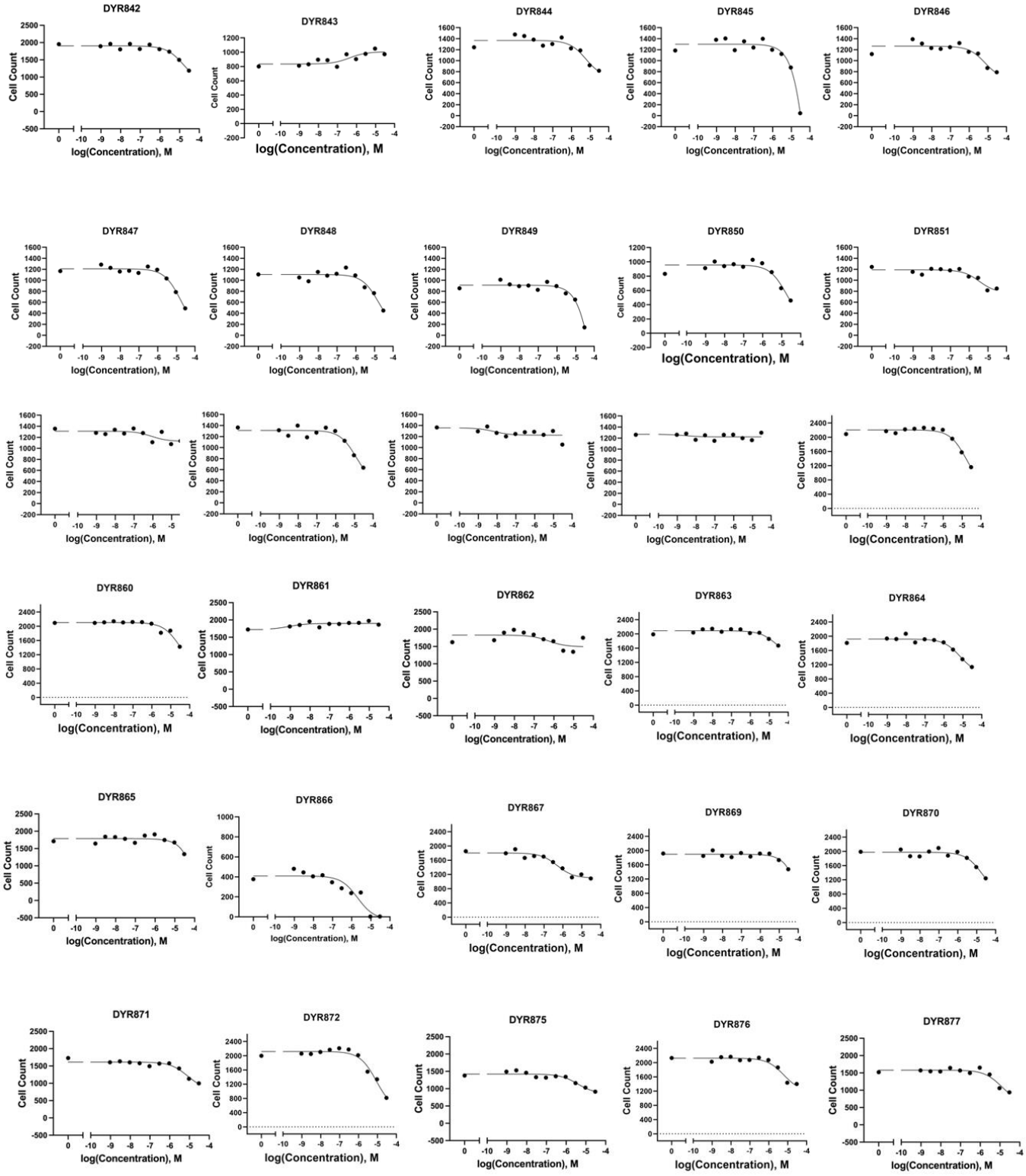

Cell Count Analysis (DYR878-DYR911)

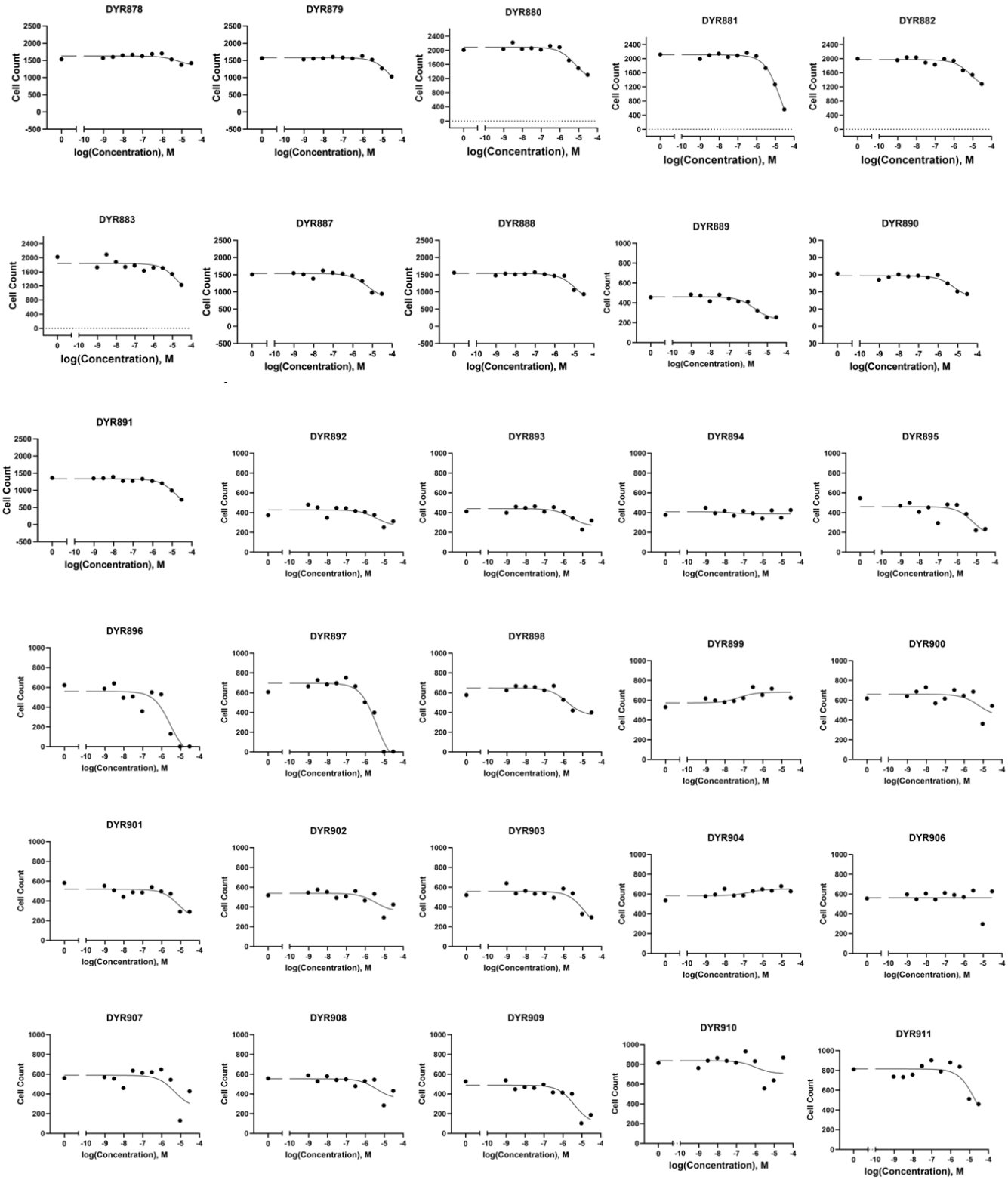

Cell Count Analysis (DYR912-CPD-A)

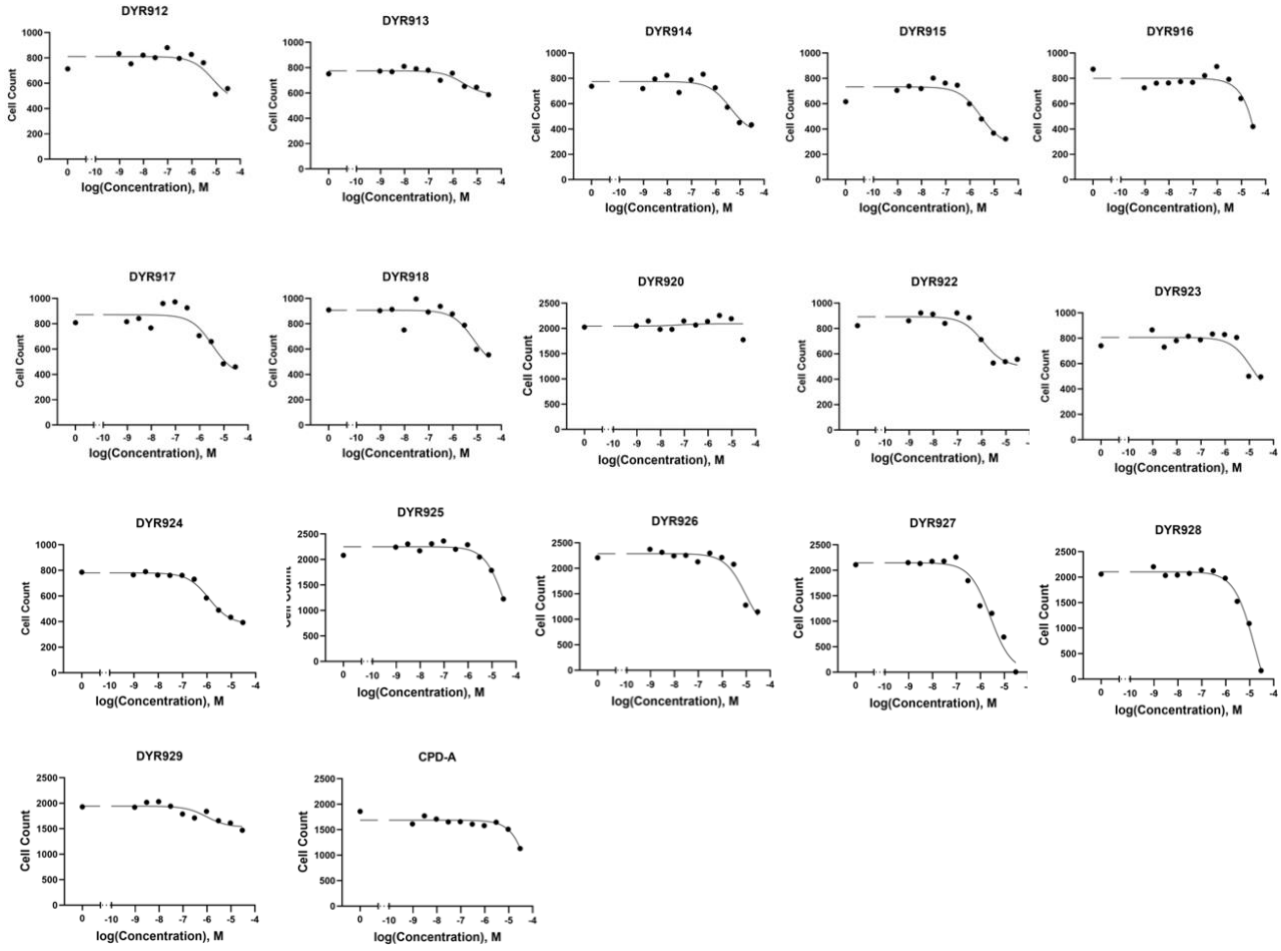

Figure 4. Cell Count Analysis Helps Determine if The Decrease of TopGFP is Due to Wnt Inhibition or Cell Death

Nuclei stained by DAPI were segmented and counted. The average of replicates was plotted on nonlinear regression curves. Cell Count analyses help determine if a decrease in TopGFP is due to Wnt inhibition and not cell death due to compound toxicity.

Compound	TopGFP EC50s uM	Cell count EC50s uM	Compound	TopGFP EC50s uM	Cell count EC50s uM	Compound	TopGFP EC50s uM	Cell count EC50s uM
DYR800	0.8071	>100	DYR848	0.0600	16.480	DYR893	0.0331	2.437
DYR807	0.1956	>100	DYR849	0.0586	>100	DYR894	1.9730	0.025
DYR808	0.3455	None	DYR850	0.3527	12.600	DYR895	0.0051	6.555
DYR810	0.0036	54.640	DYR851	0.0896	None	DYR896	2.1930	2.752
DYR811	0.7068	17.910	DYR852	0.0107	None	DYR897	2.8930	3.891
DYR812	0.1796	>100	DYR856	0.8534	12.340	DYR898	0.0027	1.463
DYR814	0.1505	>100	DYR857	^83940	None	DYR899	0.0090	0.022
DYR815	^1.920	0.001	DYR858	0.1186	None	DYR900	0.1808	5.553
DYR816	^2.713	5.499	DYR859	0.0120	16.960	DYR901	0.1026	7.739
DYR817	0.4515	None	DYR860	0.0145	29.250	DYR902	0.5683	3.440
DYR819	3.4970	0.000	DYR861	^88530	0.001	DYR903	0.3361	12.640
DYR820	0.2721	8.485	DYR862	0.8949	0.533	DYR904	1.2380	0.195
DYR821	0.0244	27.330	DYR863	0.2229	23.970	DYR906	0.2130	0.000
DYR823	4.1090	>100	DYR864	0.0800	7.155	DYR907	2.0010	4.716
DYR824	0.3806	7.380	DYR865	1.8520	>100	DYR908	0.1283	3.670
DYR825	0.0052	17.810	DYR866	0.2108	2.037	DYR909	^6.247	4.012
DYR827	^0.08112	None	DYR867	0.0066	0.500	DYR910	0.0245	0.999
DYR828	^5789	>100	DYR869	1.6660	>100	DYR911	0.1613	19.530
DYR829	9.6510	0.000	DYR870	0.2299	19.300	DYR912	0.0266	7.607
DYR830	0.2463	12.580	DYR871	0.0596	7.968	DYR913	0.0526	2.622
DYR831	0.1530	14.130	DYR872	0.0449	8.672	DYR914	0.0526	3.985
DYR832	5.2910	2.085	DYR875	0.0381	3.814	DYR915	0.0161	2.783
DYR833	0.0475	9.454	DYR876	0.0377	6.120	DYR916	0.0932	>100
DYR834	0.0930	>100	DYR877	0.2052	11.840	DYR917	0.0131	3.354
DYR835	0.2201	30.210	DYR878	0.0466	6.645	DYR918	0.1782	7.158
DYR837	^0.43	1.622	DYR879	0.0218	29.520	DYR920	0.9148	0.060
DYR838	0.2681	12.280	DYR880	0.0134	6.386	DYR922	0.0284	1.152
DYR839	1.2510	0.000	DYR881	0.5355	19.850	DYR923	0.0560	12.890
DYR840	0.1607	4.616	DYR882	0.0105	7.726	DYR924	0.0219	1.212
DYR841	4.8040	8.688	DYR883	0.2619	18.090	DYR925	0.3066	39.000
DYR842	0.1447	15.920	DYR887	0.0981	5.853	DYR926	0.0838	9.371
DYR843	^0.4891	0.422	DYR888	0.4000	12.000	DYR927	0.8498	2.622
DYR844	0.0153	5.967	DYR889	0.0652	2.135	DYR928	0.0512	16.800
DYR845	0.0787	>100	DYR890	0.0413	6.558	DYR929	0.0702	0.951
DYR846	0.0440	7.111	DYR891	0.9520	17.200	CPD-A	0.2587	274.700
DYR847	0.1723	16.740	DYR892	4.7160	3.644			

^	Represents compounds that did not reduce TopGFP to negative control
None	Represents curves that flatlined and did not fit nonlinear regression
>	Represents values greater that the recorded number have calculated EC50's higher that the maximum dose tested

Table 1. TopGFP and Cell Count EC50s of Pan-CLK/DYRK Inhibitors on HCECs with TopGFP Reporter

HCECs with TopGFP reporter were stimulated with CHIR99021 and a library of molecules synthesized to inhibit CLKs and DYRKs. TopGFP was calculated by dividing the average of GFP reporter intensities by the average of mCherry control intensities. To obtain EC50s of TopGFP and cell count, TopGFP/mCherry values and cell count were plotted on nonlinear regression curves.

The Six Most Potent Small Molecules are Tested on Four Cancer Cell Lines to Obtain Kill Curves.

Compounds DYR682, DYR726, DYR747, DYR810, DYR825, DYR860, DYR895, and DYR899 have been characterized as the most potent Wnt target gene inhibitors on healthy cells, thus far. Wnt activation was modulated by exposing HCECs to CHIR99021. This is necessary for healthy HCECs. On the other hand, cancer cell lines have mutations

that support abnormal Wnt signaling activation. To determine the potency of the top molecules against cancer cell lines, we perform kill curves using four different cancer cell lines. Our cell viability assay subjects Caco-2, HCT-116, SW480, and COLO 205 cells to an 11-dose-response treatment of eight compounds. A few cells are seeded on a 96-well culturing plate with regular media and given an overnight incubation period to allow adherence. The next day, regular media is discarded off the plates and replaced with a mix of DMEM (without fetal bovine serum, FBS) and LWRN at 1:1. The FBS is left out because we want to measure cell survival due to Wnt activation and not due to the supplementation of rich proteins and growth factors found in FBS. The addition of LWRN in the treatment is to encourage Wnt activation of the cancer lines. The pan-CLK/DYRK compounds are administered using a Tecan d300 digital dispenser at a dose-response curve ranging from concentrations of 0μM to 3μM. After treatment, the plates are placed in a 37° C- incubator for 96 hours. On the fourth day, the media with the drugs are flicked out of the plates. A mixture of Passive Lysis Buffer with Cell Titer Glo is made and added to the cells. We allow an incubation period of 15 minutes on a plate shaker at room temperature. After incubation, collect about 20μL and transfer well contents in a 384-well white microplate. A luminometer reads the luminescence released by the Cell Titer Glo. The data was obtained by calculating the mean of duplicates for each dose. Data was plotted on nonlinear regression obtained from GraphPad Prism 10.

The most potent compounds for the cell viability tests performed on the Caco-2 cell line were DYR747 and DYR810, with low cell viability at lower drug doses of 0.0392 μM and 0.0599 μM, respectively. D899 and DYR682 resulted as low performers with EC50s of 0.6428 μM and 0.3350 μM, respectively. DYR726 was the bottom-third

performer with EC50s of 0.2192 μM (Figure 5A). The compounds that performed best with the COLO-205 cell line were DYR747 and DYR895, with EC50s of 0.1118 μM and 0.5204 μM, respectively. The low performers against the COLO-205 cell line were DYR899 with an EC50 of 4.3590 μM and DYR726 with 3.5130 μM (Figure 5B). Similarly, against the SW480 cell line, DYR895 and DYR747 performed as the topmost potent compounds with EC50s of 0.0093 μM and 0.0499 μM, respectively. DYR726 was the bottom performer against the SW480 cell line (Figure 5C). Finally, for the HCT-116 cell line, DYR747 and DYR895 resulted in the top performers with EC50s of 0.046 μM and 0.45 μM, respectively. DYR899 was the weakest compound against the HCT-116 cells (Figure 5D).

A

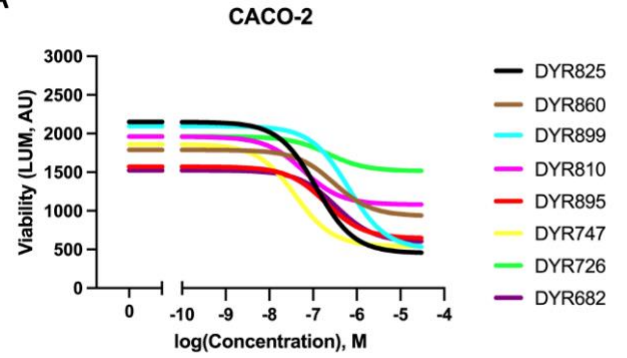

Cell lines/compounds	EC50s uM
Caco-2/825	0.1184
Caco-2/860	0.2977
Caco-2/899	0.6428
Caco-2/810	0.0599
Caco-2/895	0.1941
Caco-2/747	0.0392
Caco-2/726	0.2192
Caco-2/682	0.3350

B

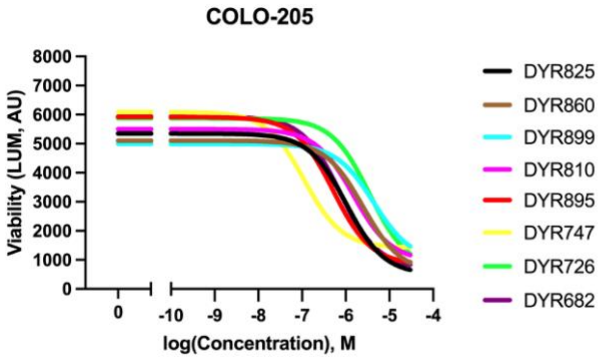

Cell lines/compounds	EC50s uM
Colo-205/825	1.0330
Colo-205/860	2.4930
Colo-205/899	4.3590
Colo-205/810	1.4950
Colo-205/895	0.5204
Colo-205/747	0.1118
Colo-205/726	3.5130
Colo-205/682	0.7417

C

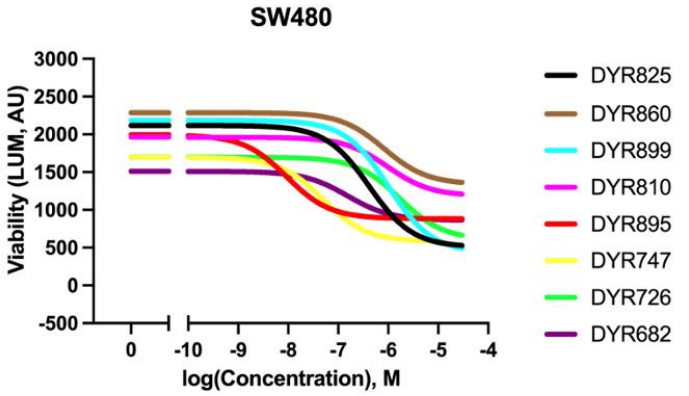

Cell lines/compounds	EC50s uM
SW480/825	0.4159
SW480/860	0.8208
SW480/899	1.0130
SW480/810	0.9690
SW480/895	0.0093
SW480/747	0.0499
SW480/726	1.6970
SW480/682	0.1536

D

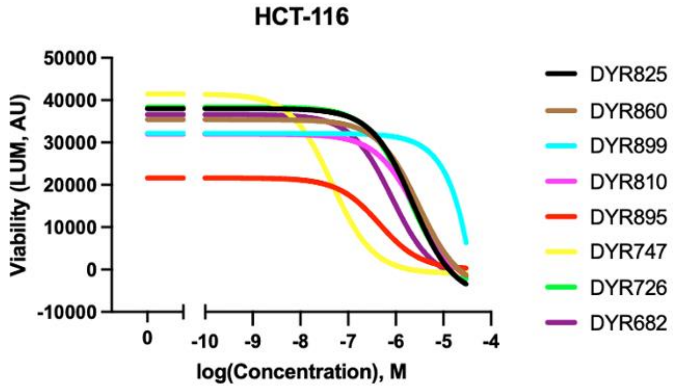

Cell lines/compounds	EC50s uM
HCT-116/825	2.2680
HCT-116/860	3.0020
HCT-116/899	1473.0000
HCT-116/810	2.7550
HCT-116/895	0.4500
HCT-116/747	0.0460
HCT-116/726	1.9150
HCT-116/682	0.8327

Figure 5. DYR747 and DYR895 are The Most Potent Small Molecules Against Cancer Cell Lines

A cell viability assay using Cell Titer Glo was performed on four cancer cell lines to obtain kill curves for the eight top pan-CLK/DYRK inhibitors with the most potent abilities to inhibit Wnt target genes obtained on the Wnt reporter assay. The four cancer cell lines were treated with the compounds on an 11-dose-response curve and were lysed and treated with Cell Titer Glo. Luminescence was read, and the average of duplicates was obtained to be graphed on nonlinear regression curves calculated using GraphPad Prism 10. ***A.*** *The two most potent compounds against the Caco-2 cancer cell line were DYR747 and DYR810, with EC50s of 0.0392 μM and 0.0599 μM, respectively. The least capable compounds were DYR899 and DYR682.* ***B.*** *The best compounds to respond against COLO-205 cells were DYR747 and DYR895. The least successful compound was DYR899.* ***C*** *&* ***D.*** *For the cell lines SW480 and HCT-116, DYR747, and DYR895 resulted in the top with the lowest concentrations to kill half of the cells.*

DYR747 and DYR810 Pan-CLK/DYRK Do Not Inhibit SRSF Phosphorylation on HCECs. Next, we attempted to unravel the function in which these drugs inhibit CLKs/DYRKs. We know CLKs' and DYRKs' primary function is phosphorylating SRSF proteins. If CLKs and DYRKs are inhibited by these drugs, then SRSF phosphorylation should also be affected by the compounds. We treated HEK293 cells with varying concentrations of top compound DYR747 and allowed an incubation period of 24 hours to immunoblot (Cabel, 2023). With an increased concentration of DYR747, we see a decreased phosphorylation of pSRSF6 and pSRSF4 but not of pSRSF5 (Figure 5A). The uniformity of pSRSF5 could be due to its lighter weight. We wanted to duplicate these results with HCECs next to DYR682, previously confirmed to reduce SRSF phosphorylation (Tam et al., 2020). With HCECs, different concentrations of DYR747 demonstrated no changes to SRSF phosphorylation, while the dephosphorylation of SRSF proteins with DYR682 was confirmed (Figure 5B). We tried another top compound, DYR810, and ultimately replicated the results we obtained with DYR747. DYR810 did not show changes in SRSF phosphorylation on HCECs, while DYR682 abilities were confirmed again (Figure 5C). To confirm the inability of DYR810 to inhibit SRSF phosphorylation, we decided to try the drug on a different cell line. We treated SW480 cells with DYR810, and in fact, the outcome was as expected- there were no changes in SRSF phosphorylation, yet DYR682 was consistent with its efficacy in decreasing SRSF phosphorylation (Figure 5D).

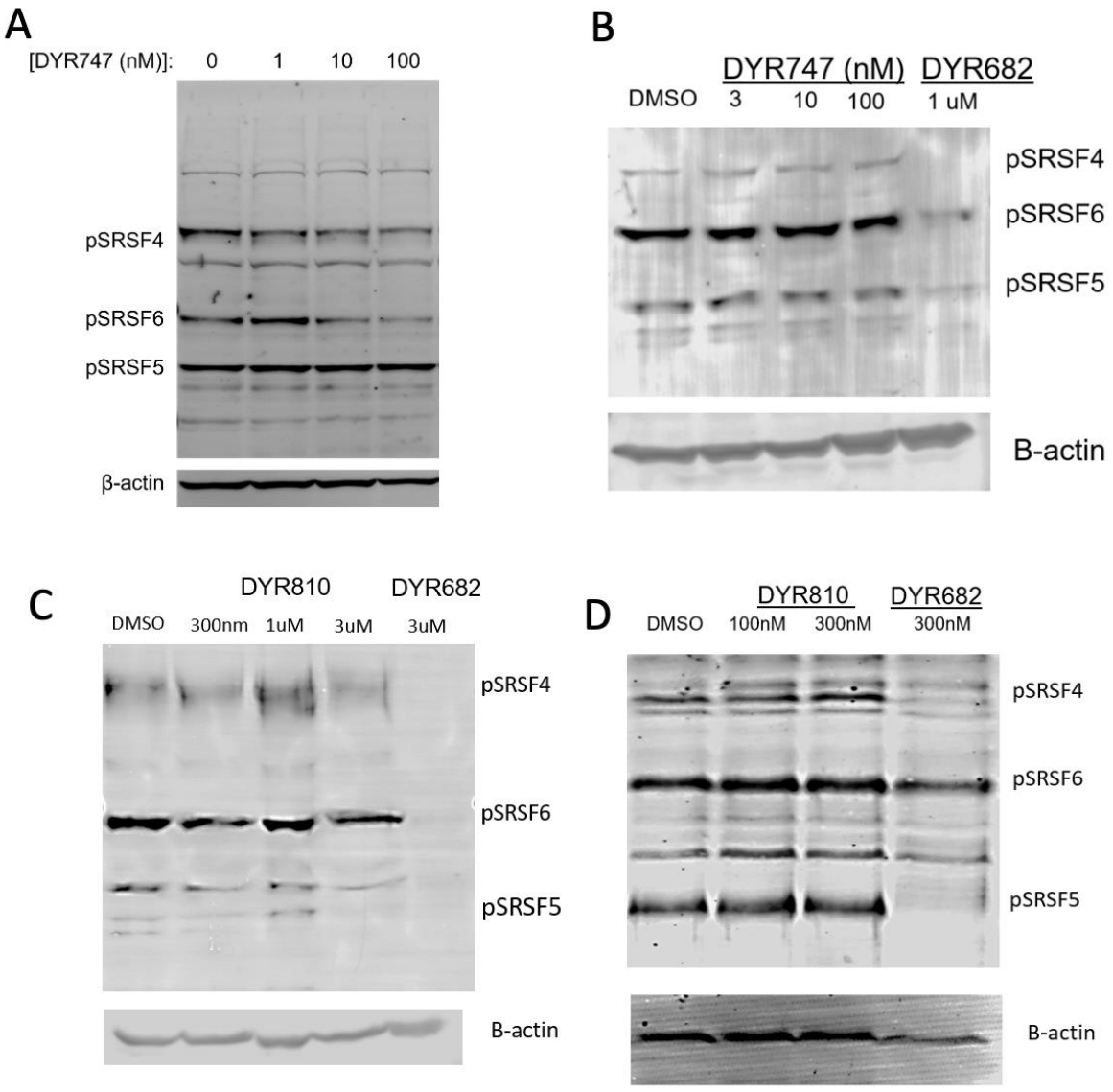

Figure 6. DYR747 and DYR810 Do Not Reduce SRSF Phosphorylation in HCECs

A. *HEK293 cells were treated with DYR747 at different concentrations to show a decline in SRSF phosphorylation. On HEK293 cells, DYR747 was able to decrease SRSF4 and SRSF6.* ***B.*** *However, when HCECs were treated with DYR747, it did not produce the same outcome. There were no changes to the phosphorylation of any SRSF variants compared to the DYR692.* ***C.*** *Another top compound, DYR810, was tested on HCECs and failed to dephosphorylate SRSF proteins. A third cell line was used to confirm that DYR810 does not decrease the SRSF phosphorylation.* ***D.*** *SW480 cells were treated with DYR810. DYR810 did not decrease SRSF phosphorylation compared to DYR682.*

Pharmacokinetics Data Demonstrate That DYR726 and DYR895 are The Best Candidates to Move Forward For Further Profiling With Organoid Models.

With pharmacokinetics (PK), we are able to observe the concentration level over time of an active chemical compound within a living organism's body. Before clinical trials, PK data is obtained since it is critical information that measures the safety and efficacy of a drug. The PK data can also help determine chemical compounds' treatment dose, frequency, and time-release profiles.

After receiving the data on the small molecules' ability to inhibit Wnt target genes, the Hulme lab obtained PK data for most of the top compounds. PK data from DYR810 and DYR860 are still to be determined. The Hulme lab has determined that it is not worth obtaining PK data for DYR825 since its surrogate compound has inferior PK data. Surrogate compounds are similar in chemical composition, and sharing surrogate data is a reliable predictor of the molecule in question – in this case, DYR825 (Tetko, 2005). Also, DYR747 was not a good candidate for bioavailability testing due to its extremely poor kinetic solubility (Table 2). Bioavailability (the amount of drug readily available in the plasma) is directly proportional to kinetic solubility and can lead to insufficient drug efficacy. DYR747 has been deemed a poor candidate for further investigation.

The PK data (and all the data obtained up to this point) for DYR682 and DYR899 has been used as points of reference against which the compounds can be assessed. DYR682 does not show the best Wnt inhibition but has excellent kinetic solubility and, therefore, an excellent bioavailability of 91% (Table 2). Although DYR682 (aka SM08502) does not have a superb clearance rate, the compound has started Phase 1 clinical trials for treating CRC, prostate cancer, and non-small cell lung cancer since November of 2021. It is estimated to be completed by July 2026 (NCBI, 2023). In the case of compound

DYR899 (aka CCT251921), mixed opinions have risen about its systemic toxicity. In 2016, Clarke et al. found severe systemic toxicity associated with DYR899 due to on-target effects, but Chen et al. disproved such claims in 2019. With kinome profiling, off-target kinase hits by the DYR899 were confirmed, possibly due to high dosage usage. The status of the investigation from the drug developers needs to be clarified for DYR899. Still, its bioavailability could be much higher at a low 30%, which leads to the conclusion that there are better candidates for further in vivo investigation (Mallinger et al., 2016).

Ultimately, we are left with compounds DYR726 and DYR895. Compound DYR895 has an excellent half-time, which is the most critical parameter of PK data since it is closely linked to clearance (metabolism rate and health indicator of the intestine). Overall, an optimal range for clearance rate is greater than 8.8μL/min/mg but less than 48μL/min/mg. DYR726 has a higher clearance than what is considered optimal, but it is lower than the clearance rate of DYR682, which is already in clinical trials (Figure 6). The bioavailability for DYR726 could be more optimal, but higher than 50% is worth testing. On the other hand, DYR895 has the best PK data available. In terms of kinetic solubility, anything above 50μg/mL is considered excellent – DYR895 has a kinetic solubility of 61μg/mL. DYR895's clearance is within the optimal range, and its bioavailability is nearly optimal at 80.5%. With this and the prior data at hand, it is appropriate to move DYR726 and DYR895 on for further assessment in organoid models. Organoid models give a more accurate representation of how normal colonic epithelium behaves with the presence of stem cells and other differentiated cells. Organoid model profiling could be a step behind pushing one of these two compounds forward to being ready for IND-enabling studies, including Good Laboratory Practice

toxicology studies (standardized studies conducted according to specific guidelines and regulations) and safety pharmacology studies.

	Pharmacokinetics data obtained from mice				
Small Molecule	**Wnt EC50 uM**	**T 1/2 (min)**	**Kinetic Solubility (ug/mL)**	**Clearance (int) (uL/min/mg)**	**Bioavailability (F) %**
DYR682	0.204	13.6	93.4	93.4	91
DYR726	0.041	40.7	68	73.3	57.1
DYR747	0.004	6.1	<0.627	228.7	N/A
DYR895	0.005	71.5	61	19.4	80.5
DYR899	0.008	46.8	67.4	72	30

Table 2. PK Data Reveal Candidacy For Compounds to Move Forward For Further Assessments

Pharmacokinetic data along with Wnt EC50 reveal the compounds' candidacy to move on to further profiling. DYR682 is currently in phase 1 clinical trials. DYR747 solubility rate and half time is suboptimal for bioavailability testing. There are different opinions about the general toxicity of DYR899, but a low bioavailability percentage could be insufficient for clinical trials. DYR726 and DYR895 have great solubility rates.

Figure 7. DYR726 and DYR895 Move Forward for Profiling in Organoid Models

DYR726 and DYR895 both have excellent kinetic solubility and Wnt inhibition EC50s. DYR895 has a better bioavailability percentage and intestinal clearance, making it a much more promising compound than DYR726. Nonetheless, both compounds qualify for further biological assessment in organoid models.

Discussion

CLK3 further stimulates Wnt target gene expression, increasing cell proliferation and uncontrolled differentiation, leading to disease. It has been shown that the overexpression of CLK3 leads to a poor prognosis in CRC. Since targeting the Wnt signal pathway, in general, would be harmful to multiple body systems, targeting unregulated kinases like the CLK family instead is an essential task in the development of therapeutics for CRC.

Here, we tested 107 novel small molecules developed to inhibit CLK and DYRKs, which are kinases similar in structure and function. Using an 11-dose-response curve, we examined TopGFP analysis, and in conjunction with cell count analysis, we narrowed down to six potent pan-CLK/DYRK inhibitors. These six compounds have the lowest TopGFP EC50s that were not influenced by cell death. DYR726, DYR747, DYR810, DYR825, DYR860, and DYR895 had excellent Wnt inhibition. These compounds were further tested in a cell viability assay against cancer cell lines- DYR682 and DYR899 were used as benchmarks. In the cell viability tests, DYR747 and DYR895 were the top performers, killing the most cancer cells at lower concentrations of the compounds. Both compounds had excellent EC50's in the kill curves, showing their efficacy in killing cancer cells. DYR825 performed similarly to DYR682, both averaging performances in third place. DYR726 and DYR860 tied in fourth place, putting DYR899 as the worst performer against the four cancer cell lines.

There is still more to unravel about how these novel small molecules work. We know these compounds are pan-CLK/DYR inhibitors, but it is not clear how they inhibit CLKs and DYRKs. A small attempt was made to find a substrate to which these drugs act upon. When immunoblotting for SRSF phosphorylation by treating HCECs with DYR747

and DYR810, not much information was gained. DYR747 reduced the phosphorylation of HEK293 cells but not of HCECs. DYR810 could not effectively reduce SRSF phosphorylation of HCECs or cancer cell line SW480. What we were able to confirm is that DYR682 is very efficient at completing the task of SRSF phosphorylation reduction consistently in both HCECs and SW480 cells. This leaves us with more questions than answers about how these small molecules behave; therefore, further investigation will need to be done to understand how these small molecules act on CLK and DYRKs.

Additionally, the compounds' efficacy at inhibiting Wnt target genes and killing cancer cells are not the only relevant parameters. Pharmacokinetic data performed on mice were obtained on compounds to understand the behavior of the compound in a living organism. According to the PK data, DYR825 and DYR727 have been discarded for further assessment due to poor surrogate compound data and poor kinetic solubility, respectively. DYR726 and DYR895 are the best candidates for further investigation in organoid models. Also, we have yet to analyze the PK data of DYR810 and DYR860 (pending now). DYR895 data is by far the most superior compound out of the 107 small molecules considered. It is superior to DYR682, which has been in clinical trials since 2021. We are excited about DYR895's continued superb performance and confidently trust that FDA approval for clinical trials is in the near future.

Experimental Procedures

Wnt Reporter Assay

Human colonic epithelial cells (HCECs) were used for this experiment. They were acquired courtesy of the Jerry Shay lab from UT Southwestern. HCECs were designed to report TopGFP reporter when the Wnt signaling pathway is activated. The media used to culture HCECs is DMEM treated with 10% FBS, 1% Glutamax, and 1% penicillin/streptomycin at an incubation environment of 37° Celsius and 5% CO_2.

To initiate the Wnt reporter assay cells are grown and counted to seed 2000-2500 cells per well in a 384-well black SCREENSTAR imaging microplate. The cells on the microplates are incubated overnight to allow adherence. The cells of half of the plate are treated the following day with 10μM of CHIR99021 (Sigma-Aldrich), a Wnt activator via GSK3 inhibition. The other half of the wells are used as a control with 10μM of DMSO. Soon after, DYR compounds are administered using a Tecan d300 digital dispenser at a dose-response curve with concentrations ranging from 0μM to 30μM. After these treatments, the plates are placed in a 37° C-incubator for 24 hours. Cells are fixed the next day with 4% paraformaldehyde/sucrose solution for 10 minutes. Cells are then permeabilized for 10 minutes with 0.1% triton-x in PBS and finally stained for DAPI for 30 minutes at room temperature in the dark. DAPI is washed with PBS and fresh PBS is added to make the plate ready for imaging. For imaging a Nikon Ti2 Eclipse microscope was used under the appropriate wavelengths for DAPI, GFP, and mCherry. Nikon Elements Software was used for analysis. The nuclei of the cells were segmented based on DAPI. Mean object intensity per cell for TopGFP and mCherry are measured. Wnt activity is calculated by dividing the mean intensity of TopGFP by the mean intensity of

mCherry. EC50's and curves were plotted and calculated with Jupyter and GraphPad Prism 10 software.

Immunoblotting

After treated cells were incubated for 24 hours, cells were washed in cold PBS. A standard RIPA buffer was used and incubated on ice for 15 minutes to lyse the cells. Lysates were centrifuged at 17,000 rcf at 4°C for 20 minutes so the protein lysate would separate from cells. Thermo-Fisher Scientific Pierce BCA Protein Assay kit was used to determine the concentration of each lysate condition. Lysate samples were loaded onto standard 10%, 1.5mm SDS-Page gels and transferred onto PVDF membranes. Membranes were blocked with 10% milk in PBS for 30 minutes at room temperature on a rocker. Primary antibodies were added to membranes to incubate overnight at 4°C on a rocker. The next day the membranes were washed with TBST for 5 minutes on a rocker three times. Secondary antibodies were diluted at 1:15,000 with Odyssey Blocking Buffer and 0.05% Tween 20. Incubation of the secondary antibody was allowed for 1 hour at room temperature on a rocker. Membranes were washed three times again for 5 minutes with TBST. Membranes were left to sit in DDI water for storage until imaged. After the image is deemed appropriate primary antibody for loading control (β-actin) is loaded onto the membrane for an hour at room temperature, three 5-minute washes with TBTS follow, to finish with loading control secondary antibody.

Antibodies used for Immunoblotting.

Antibodies	Vender	Catalog Number
B-actin Ms	Cell Signaling Technology	3700S
B-actin Rb	Cell Signaling Technology	4970S
p-SRSF	EMD Millipore	MABE50
IRDye 800CW, goat anti-Ms	LI-Cor	926-32210
IRDye 800CW, goat anti-Rb	LI-Cor	926-32211
IRDye 680RD, goat anti-Ms	LI-Cor	926-68070
IRDye 680RD, goat anti-Rb	LI-Cor	926-68071

Cell Viability Assay

Cancer cell lines are grown and counted to seed approximately 500 cells per well for every cell line in 96-well tissue culture-treated microplates. The cells on the microplates are incubated overnight to allow adherence. The next day regular media is flicked off the plates and replaced with a concoction of media (without FBS) and LWRN at 1:1 is added to the wells. DYR compounds are administered using a Tecan d300 digital dispenser at a dose-response curve ranging from concentrations of 0μM to 3μM. After treatment, the plates are placed in a 37° C- incubator for 96 hours. On the fourth day, the media with the drugs are flicked out of the plates. A mixture of Passive Lysis Buffer with Cell Titer Glo at 9:1 is made to add 50μL to each. We allow an incubation period of 15 minutes on the plate shaker. After incubation, collect about 20μL and place in a 384-well white microplate. A luminescent microplate reader reads the luminescence.

References

1. World Health Organization. (2023). *Colorectal cancer*. World Health Organization. https://www.who.int/news-room/fact-sheets/detail/colorectal-cancer.

2. American Cancer Society. (2023). *Colorectal Cancer Statistics: How Common Is Colorectal Cancer?"* https://www.cancer.org/cancer/types/colon-rectal-cancer/about/key-statistics.html.

3. Kuipers, E. J., Grady, W. M., Lieberman, D., Seufferlein, T., Sung, J. J., Boelens, P. G., *et al.* (2015). Colorectal cancer. *Nature reviews. Disease primers*, *1*, 15065. https://doi.org/10.1038/nrdp.2015.65.

4. Nusse, R., Brown, A., Papkoff, J., Scambler, P., Shackleford, G., McMahon, A., *et al.* (1991). A new nomenclature for int-1 and related genes: the Wnt gene family. *Cell*, *64*(2), 231.

5. Nusse, Roel. April 2023. "Wnt Signaling." Wnt signaling | The Wnt Homepage. https://web.stanford.edu/group/nusselab/cgi-bin/wnt/node/261.

6. MacDonald, B. T., Tamai, K., & He, X. (2009). Wnt/beta-catenin signaling: components, mechanisms, and diseases. *Developmental cell*, *17*(1), 9–26.

7. Schatoff, E. M., Leach, B. I., & Dow, L. E. (2017). Wnt Signaling and Colorectal Cancer. *Current colorectal cancer reports*, *13*(2), 101–110.

8. Cheng, H. C., Qi, R. Z., Paudel, H., & Zhu, H. J. (2011). Regulation and function of protein kinases and phosphatases. *Enzyme research*, *2011*, 794089. https://doi.org/10.4061/2011/794089

9. Lindberg, M. F., & Meijer, L. (2021). Dual-Specificity, Tyrosine Phosphorylation-Regulated Kinases (DYRKs) and cdc2-Like Kinases (CLKs) in Human Disease, an Overview. *International Journal of Molecular Sciences*, *22*(11), 6047.

10. Aubol, B. E., Plocinik, R. M., Hagopian, J. C., Ma, C. T., McGlone, M. L., Bandyopadhyay, R., *et al.* (2013). Partitioning RS domain phosphorylation in an SR protein through the CLK and SRPK protein kinases. *Journal of molecular biology*, *425*(16), 2894–2909.

11. Song, M., Pang, L., Zhang, M., Qu,Y., Vaughn Laster, K., & Dong, Z.(2023).Cdc2-like kinases: structure, biological function, and therapeutic targets for diseases. *Signal Transduction Target Therapy,* **8**, 148.

12. Thorne, C. A., Wichaidit, C., Coster, A. D., Posner, B. A., Wu, L. F., & Altschuler, S. J. (2015). GSK-3 modulates cellular responses to a broad spectrum of kinase inhibitors. *Nature chemical biology*, *11*(1), 58–63.

13. Cabel, C.R. (2023) *Identification and characterization of CLK3 in the colonic epithelium as a regulator of the Wnt pathway.* Ph.D dissertation, University of Arizona.

14. Human Protein Atlas. (n.d.). *DATA*. Expression of CLK3 in colorectal cancer - The human protein atlas. https://www.proteinatlas.org/ENSG00000179335-CLK3/pathology/colorectal+cancer.

15. Berginski M.E., Moret, N., Liu, C., Goldfarb, D., Sorger, P.K., & Gomez, S.M. (2021). The Dark Kinase Knowledgebase: an online compendium of knowledge and experimental results of understudied kinases. *Nucleic Acids Research*. Volume 49, Issue D1, D529–D535.

16. Tam, B. Y., Chiu, K., Chung, H., Bossard, C., Nguyen, J. D., Creger, E., Eastman, B. W., Mak, C. C., Ibanez, M., *et al.* (2020). The CLK inhibitor SM08502 induces anti-tumor activity and reduces Wnt pathway gene expression in gastrointestinal cancer models. *Cancer Letters*, *473*, 186–197.

17. Tetko, I. V., Abagyan, R., & Oprea, T. I. (2005). Surrogate data--a secure way to share corporate data. *Journal of computer-aided molecular design*, *19*(9-10), 749–764.

18. NCBI. (2022). *A Study Evaluating the Safety, Pharmacokinetics, and Preliminary Efficacy of Orally Administered SM08502 Combined With Hormonal Therapy or Chemotherapy in Subjects With Advanced Solid Tumors*. CTG Labs. https://clinicaltrials.gov/study/NCT05084859

19. Clarke P.A., Ortiz-Ruiz M.J., TePoele R., Adeniji-Popoola O., Box G., Court W., Czasch S., El Bawab S., Esdar C., Ewan K., et al. (2016). Assessing the mechanism and therapeutic potential of modulators of the human mediator complex-associated protein kinases. *eLife*. doi: 10.7554/eLife.20722

20. Chen, M., Li, J., Liang, J., Thompson, Z. S., Kathrein, K., Broude, E. V., & Roninson, I. B. (2019). Systemic Toxicity Reported for CDK8/19 Inhibitors CCT251921 and MSC2530818 Is Not Due to Target Inhibition. *Cells*, *8*(11), 1413.

21. Mallinger, A., Schiemann, K., Rink, C., Stieber, F., Calderini, M., Crumpler, S., Stubbs, M., Adeniji-Popoola, O., Blagg, J., *et al.* (2016). Discovery of potent, selective, and orally bioavailable small-molecule modulators of the mediator complex-associated kinases CDK8 and CDK19. *Journal of Medicinal Chemistry*, *59*(3), 1078–1101.